Quarterly Technical Report

Growth, Characterization and Device Development in
Monocrystalline Diamond Films
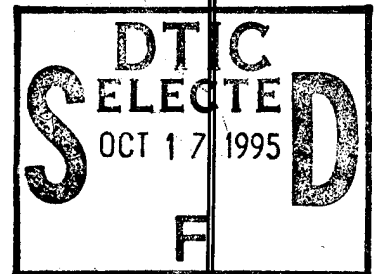
R. F. Davis, J. T. Glass, R. J. Nemanich* and Z. Sitar
P. K. Baumann, S. P. Bozeman, M. T. McClure, and B. L. Ward
North Carolina State University
c/o Materials Science and Engineering Department
*Department of Physics
Raleigh, NC 27695

19951013 030

September, 1995

DTIC QUALITY INSPECTED 8

REPORT DOCUMENTATION PAGE

1. AGENCY USE ONLY (Leave blank)	2. REPORT DATE	3. REPORT TYPE AND DATES COVERED
	September, 1995	Quarterly Technical 7/1/95–9/30/95

4. TITLE AND SUBTITLE

Growth, Characterization and Device Development in Monocrystalline Diamond Films

5. FUNDING NUMBERS

s400003srr14
1114SS
N00179
N66005
4B855

6. AUTHOR(S)

R. F. Davis, J. T. Glass, R. J. Nemanich and Z. Sitar

7. PERFORMING ORGANIZATION NAME(S) AND ADDRESS(ES)

North Carolina State University
Hillsborough Street
Raleigh, NC 27695

8. PERFORMING ORGANIZATION REPORT NUMBER

N00014-93-I-0437

9. SPONSORING/MONITORING AGENCY NAMES(S) AND ADDRESS(ES)

Sponsoring: ONR, Code 312, 800 N. Quincy, Arlington, VA 22217-5660
Monitoring: Admin. Contracting Officer, ONR, Regional Office Atlanta
101 Marietta Tower, Suite 2805
101 Marietta Street
Atlanta, GA 30323-0008

10. SPONSORING/MONITORING AGENCY REPORT NUMBER

11. SUPPLEMENTARY NOTES

12a. DISTRIBUTION/AVAILABILITY STATEMENT

Approved for Public Release; Distribution Unlimited

12b. DISTRIBUTION CODE

13. ABSTRACT (Maximum 200 words)

Electron emission has been observed on three types of diamond samples: films deposited on both Si(100) wafers and on individual Mo tips via plasma chemical vapor deposition (CVD) and also on the Mo tips via dielectrophoresis of diamond powder. In the first sample type, ultraviolet photoemission spectroscopy showed that the samples exhibited a negative electron affinity after exposure to a hydrogen plasma. Secondary electron emission yields varied from 2.2 to 9.2. Field emission current-voltage measurements showed threshold voltages ranging from 28 to 84 V/μm and effective emission barrier heights from 0.15 to 0.33 eV. The film with the highest secondary yield also exhibits the lowest emission threshold. In the last two sample types, transmission and scanning electron microscopies revealed a significant amount of diamond on the tips of the Mo emitters. The field emission characteristics were investigated before and after diamond deposition. The CVD diamond coated emitters exhibited a significant increase in emission current. A possible mechanism to explain the current enhancement by diamond powder coated Mo emitters has been presented.

14. SUBJECT TERMS

diamond films, chemical vapor deposition, dielectrophoresis, silicon wafers, molybdenum tips, electron emission, negative electron affinity, ultraviolet photoemission spectroscopy

15. NUMBER OF PAGES

21

16. PRICE CODE

17. SECURITY CLASSIFICATION OF REPORT	18. SECURITY CLASSIFICATION OF THIS PAGE	19. SECURITY CLASSIFICATION OF ABSTRACT	20. LIMITATION OF ABSTRACT
UNCLAS	UNCLAS	UNCLAS	SAR

Table of Contents

Accesion For		
NTIS CRA&I	☑	
DTIC TAB	☐	
Unannounced	☐	
Justification		
By		
Distribution /		
Availability Codes		
Dist	Avail and / or Special	
A-1		

I. Introduction

Diamond as a semiconductor in high-frequency, high-power transistors has unique advantages and disadvantages. Two advantages of diamond over other semiconductors used for these devices are its high thermal conductivity and high electric-field breakdown. The high thermal conductivity allows for higher power dissipation over similar devices made in Si or GaAs, and the higher electric field breakdown makes possible the production of substantially higher power, higher frequency devices than can be made with other commonly-used semiconductors.

In general, the use of bulk crystals severely limits the potential semiconductor applications of diamond. Among several problems typical for this approach are the difficulty of doping the bulk crystals, device integration problems, high cost and low area of such substrates. In principal, these problems can be alleviated via the availability of chemically vapor deposited (CVD) diamond films. Recent studies have shown that CVD diamond films have thermally activated conductivity with activation energies similar to crystalline diamonds with comparable doping levels. Acceptor doping via the gas phase is also possible during activated CVD growth by the addition of diborane to the primary gas stream.

The recently developed activated CVD methods have made feasible the growth of polycrystalline diamond thin films on many non-diamond substrates and the growth of single crystal thin films on diamond substrates. More specifically, single crystal epitaxial films have been grown on the {100} faces of natural and high pressure/high temperature synthetic crystals. Crystallographic perfection of these homoepitaxial films is comparable to that of natural diamond crystals. However, routes to the achievement of rapid nucleation on foreign substrates and heteroepitaxy on one or more of these substrates has proven more difficult to achieve. This area of study has been a principal focus of the research of this contract.

At present, the feasibility of diamond electronics has been demonstrated with several simple experimental devices, while the development of a true diamond-based semiconductor materials technology has several barriers which a host of investigators are struggling to surmount. It is in this latter regime of investigation that the research described in this report has and continues to address.

In this reporting period, sample preparation and associated electron emission studies have been conducted on three different types of diamond samples, namely, films deposited on both Si(100) wafers and on individual Mo tips via plasma chemical vapor deposition (CVD) and also on the Mo tips via dielectrophoresis of diamond powder. All sample types exhibited significant emission. A negative electron affinity was observed on the first sample type after exposure to a hydrogen plasma. The following sections are self-contained in that they present an introduction, the experimental procedures, results and discussion, summary and indications of future research for the given research thrust.

II. Field Emission from Diamond Coated Molybdenum Field Emitters[1]

W. B. Choi, J. Liu[a] , M. T. McClure, A. F. Myers, V. V. Zhirnov[b], J. J. Cuomo and J. J. Hren

Abstract

Diamond deposition on single Mo field emitters was accomplished by two methods: microwave plasma CVD and a dielectrophoresis diamond powder coating method. TEM and SEM observation revealed a significant amount of diamond on tip of the Mo emitters. The field emission characteristics were investigated before and after diamond deposition. Field emission from the diamond coated emitters exhibited significant increase in emission current. We suggest a possible mechanism to explain the current enhancement by diamond powder coated Mo emitters.

A. Introduction

Micro-fabricated molybdenum field emitters have been used in developing the next generation of vacuum microelectronics and flat panel display devices.[1,2] To improve the performance and enhance the emission current of field emitters, diamond deposition on Mo and Si has been studied.[3,4,5] Diamond showed excellent thermal, chemical, properties and the negative electron affinity (NEA) effects. Photoemission experiments demonstrated the NEA property of the hydrogen terminated (111)[6] and (100)[7] surfaces of CVD diamond. There have been several studies of the field emission properties of CVD diamond on metal cathodes. Liu *et al.* reported that CVD diamond coated W tips showed very high hardness and good electrical conductivity for STM studies.[8] Xu *et al.* shows electron emission from CVD diamond films deposited on an Mo substrate.[9] Mousa reported that ZnO coated W tip shows good current stability and high brightness.[11] Until now, no field emission data from diamond coated metal tip has been published. In this article, the result of field emission studies from CVD diamond and high pressure synthetic diamond powder coated Mo emitters reported. In addition, we suggest a possible mechanism to explain the current enhancement by diamond powder coated Mo emitters.

B. Experimental Procedure

Mo Emitter Tip Preparation. The single emitter tip was made from 99.95% pure 0.125mm Mo wire. A short length of wire was mounted in a Cu tube and then etched electrolytically in

concentrated potassium hydroxide solution. 10 volts dc was applied between the Mo cathode and a Pt as the anode.

Growth of CVD Diamond. To increase the number of diamond nucleation sites, tips were treated in an ultrasonic bath of diamond powder suspended in ethanol for less than 5min. This scratching process was found to be an effective technique to nucleate a diamond on metal tip end. The samples were then loaded into a CVD chamber and H_2 plasma treated at a pressure of 25Torr. After a cleaning step, diamond was grown on the Mo needles using deposition times up to 45 minutes and at a pressure of about 25 Torr with CH_4/H_2 ratio of 0.2%. The tips fabricated in this manner are referred as Mo(1) tips.

Diamond Coating by Dielectrophoresis. Dielectrophoresis is the movement of neutral matter in the presence of a nonuniform electric field.[5,12] A nonuniform field occurred in the diamond suspension due to the sharpness of the tip, this field gives a net force impelling the diamond particle toward the region of strongest field of the tip. A suspension of diamond powder was prepared by ultrasonically mixing diamond powder and ethanol. The Mo tip was dipped into this suspension and biased positively. An applied voltage was 6 to 12 V. Diamond coatings on the Mo tip were deposited preferentially by this technique. The tips fabricated in this manner are referred as Mo(2) tips.

Microstructural Characterization. The morphology of the diamond coatings was studied by a scanning electron microscope (JEOL 6400 field emission SEM). High resolution transmission electron microscopy (HRTEM) investigations were performed by means of a Topcon 002B TEM. Raman spectra were obtained on an Instruments SA U1000 apparatus using an argon laser with a microprobe. The laser can be focused onto a surface area of about a few μm diameter on the samples. The laser power used was 100-200mW.

Field Emission Experiments. The field emission characteristics of the Mo emitters were investigated before and after diamond deposition by means of an ultra high vacuum FIM/FEM system. The measurements were carried out at room temperature and under a vacuum of 10^{-9} Torr or better. To avoid errors from different tip shapes, the field emission characteristics were carried out before and after diamond coating on the same Mo tip.

C. Results and Discussion

Electron Microscopy Studies. It was found that diamond did not nucleate on the very tip end under negative substrate bias during microwave plasma chemical vapor deposition (MPCVD). The negative substrate bias technique is proven technique for nucleation enhancement on planar surfaces (nucleation density of Si ~ 5×10^{10} cm^{-2}).[20] We suggest one possible explanation is electrons ejected from the tip end dissociate the CH_3 radicals, or positively charged tip end by Jellium effect. The formation of stable diamond nuclei was

obtained by surface scratching and the growth procedures described above. Figure 1 shows a typical Mo emitters before and after CVD diamond. The size of the diamond grains was found to range from a tens of nm to hundreds of nm. The size is ten times bigger than that deposited on Si tips, which described in our previous paper.[3] The Raman spectra showed a sharp peak at 1332cm^{-1} characteristic of sp^3 diamond bonding with a long-range order, while the broad peak around 1500cm^{-1} was due to the disordered sp^2 bonded carbon component arising from graphitic material, as shown in Fig. 2.[13] This result showed good agreement with TEM analysis, see Fig. 3. The TEM micrographs showed many nanometer size diamond particles mixed with graphitic material and the ring pattern was consistent with diamond and a carbide layer.

Figure 4 shows Mo emitters before and after the dielectrophoresis diamond powder coating. The size of the diamond grains was found to range from 20nm to 200nm. The diamond particles remained on the emitter surface even after I-V characterization (Fig. 4b). The calculated sticking force of diamond particles on the tip is about one order of magnitude stronger than the Coulomb force.[12] Raman measurements show a sharp peak at 1324cm^{-1} which is characteristic of twinned sp^3 diamond bonding with no sp^2, see Fig. 5. This result agrees well with TEM electron diffraction analysis, which shows only polycrystalline diamond ring patterns (Fig. 6).

(a)   (b)
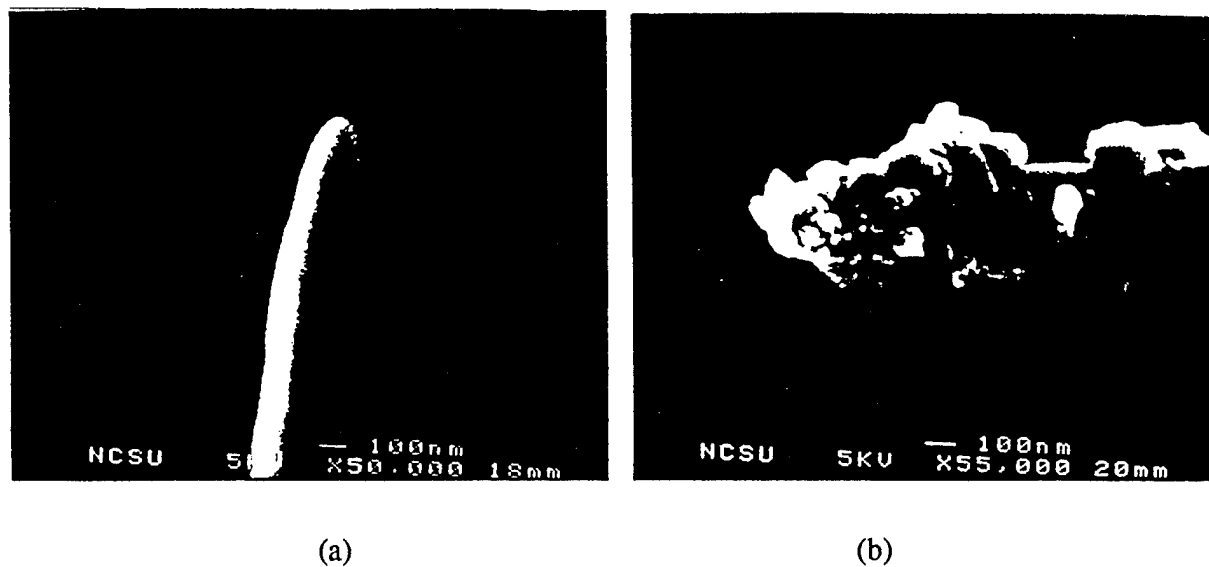
Figure 1.   SEM micrographs of molybdenum emitter (a) before and (b) after CVD diamond deposition.
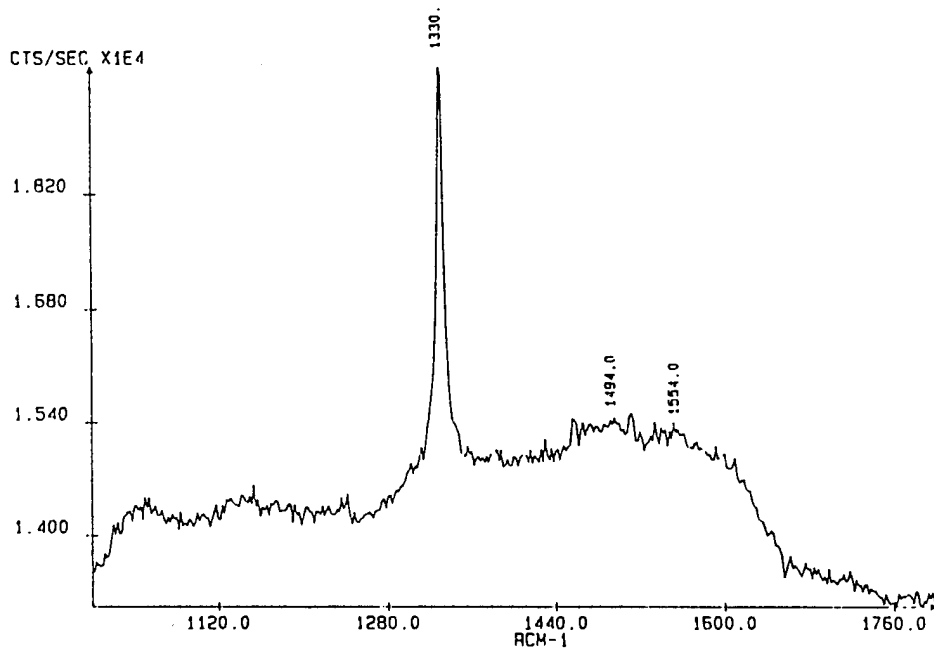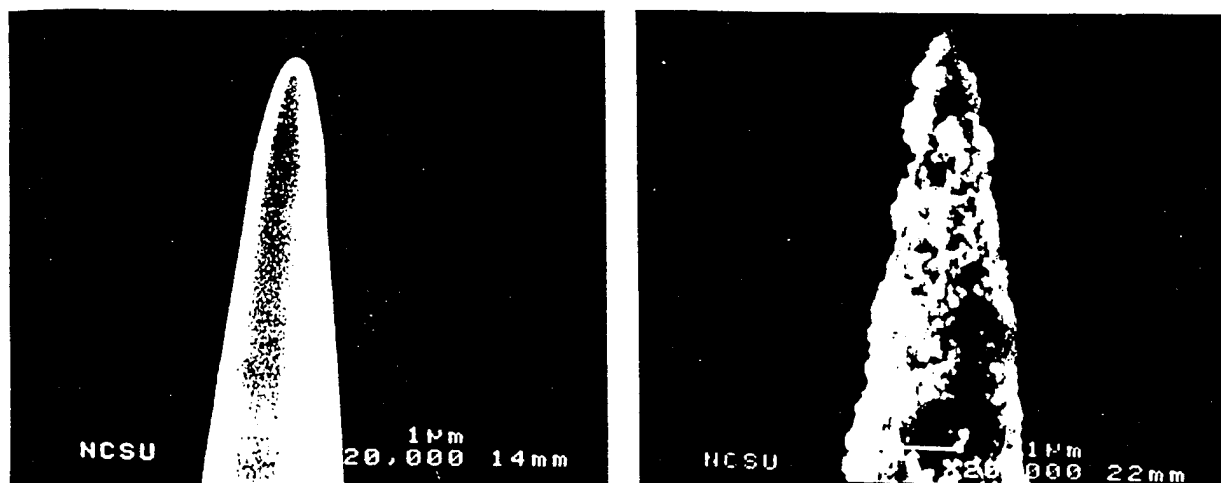
Figure 2.   Raman spectrum of CVD diamond coated Mo emitter showing peaks characteristic of diamond (1330 cm^{-1}) and sp^2-bonded carbon (1494 cm^{-1} and 1554 cm^{-1}).

Figure 3.   TEM micrograph of CVD diamond coating showing diamond particles mixed with graphitic material. Inset is a diffraction pattern displaying a ring pattern consistent with diamond and a carbide layer.

5

(a)   (b)

Figure 4.   SEM micrographs of molybdenum emitter (a) before and (b) after
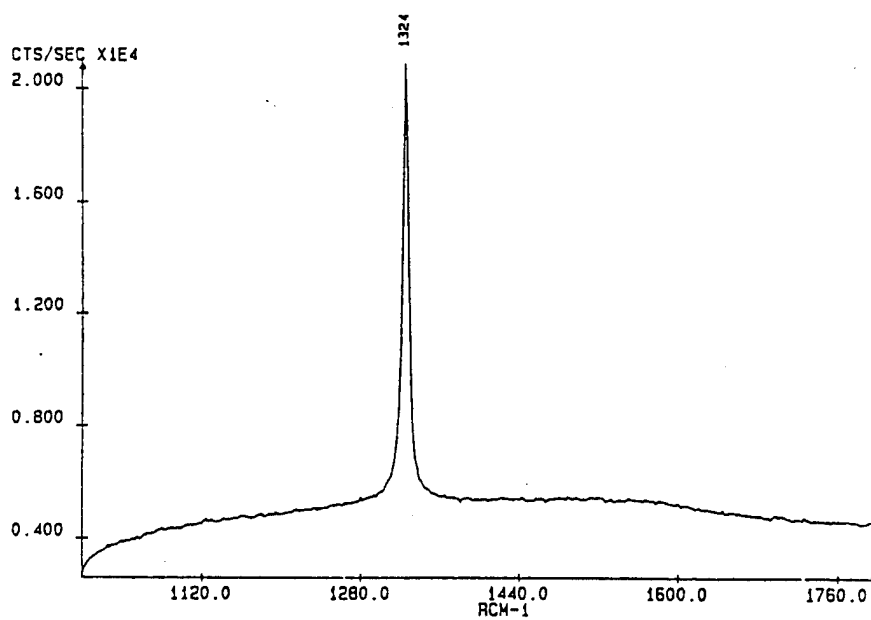   dielectrophoresis deposition of diamond powders.

Figure 5.   Raman spectrum of diamond powder coated Mo emitter showing peaks
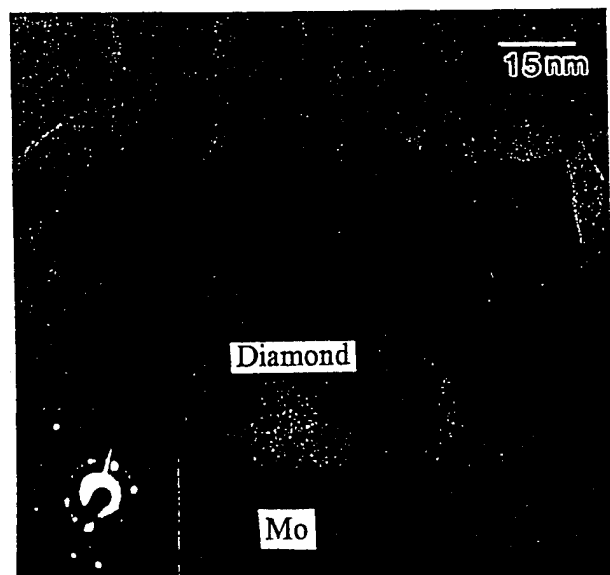   characteristic of twinned diamond (1324 cm^{-1}).

6

Figure 6.   TEM micrograph of diamond powder coating showing only diamond particles. Inset is a diffraction pattern displaying a ring pattern consistent with diamond particles.

Electrical Characteristics. Field emission current-voltage measurements were performed on diamond coated Mo emitters, and uncoated pure Mo(1) and Mo(2) different tip radius emitters were also studied under the same conditions for comparison. To avoid errors from different tip shapes, the field emission characteristics were carried out on the same Mo tip. Two sets of I-V curves, One from a CVD-diamond coated Mo single emitter and the other from a diamond powder coated Mo single emitter are shown in Fig. 7a and Fig. 8a respectively, and were compared to pure Mo emitter. Diamond coated Mo emitters appear to have a lower turn-on voltage and a higher increase in current than the pure Mo emitter. Fowler-Nordheim plots corresponding to each type of diamond coatings are compared and shown in Fig. 7b, Fig. 8b, respectively. The field emission data obtained from our measurements were calculated from Fowler-Nordheim plots using the slope and intercept. Our measured results for different diamond types of emitters are presented in Table I. The different emitting area of Mo(1) and Mo(2) probably comes from the differences of shape and tip radius of curvature 300Å and 600Å. Cuttler *et al.* suggested that Fowler-Nordheim theory can not be applied on an small tip radius.[14]

For the CVD-diamond coated emitter, the calculated emitting area (α) is less than a clean Mo emitter. This result can be explained by the thick contamination layer on CVD-diamond surfaces which is shown in TEM images and explained it previous section, but a full explanation is being sought.
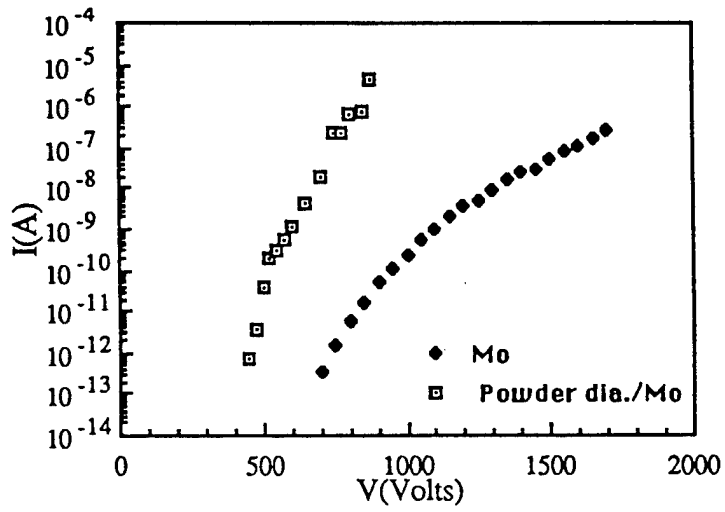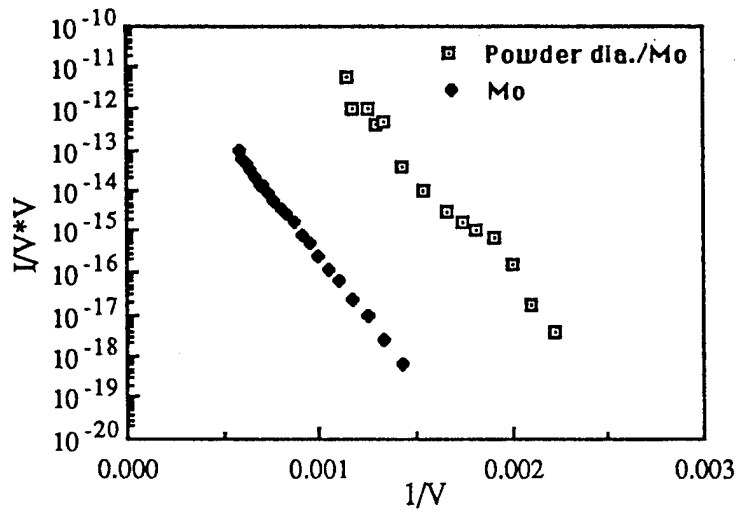
7
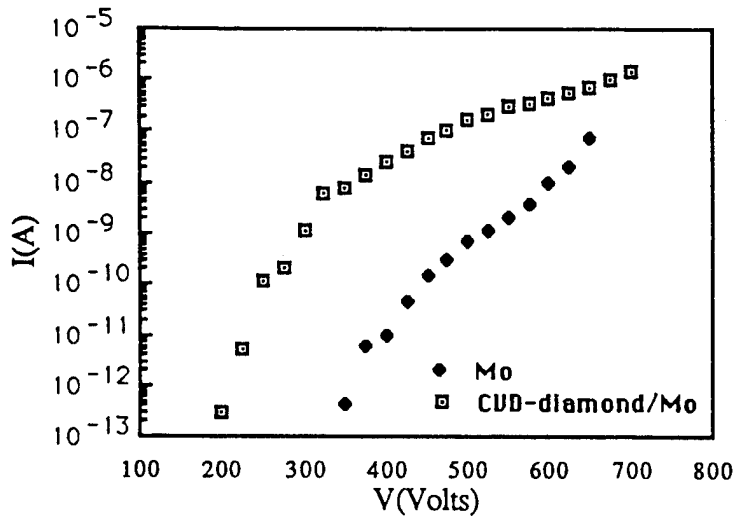
(a)
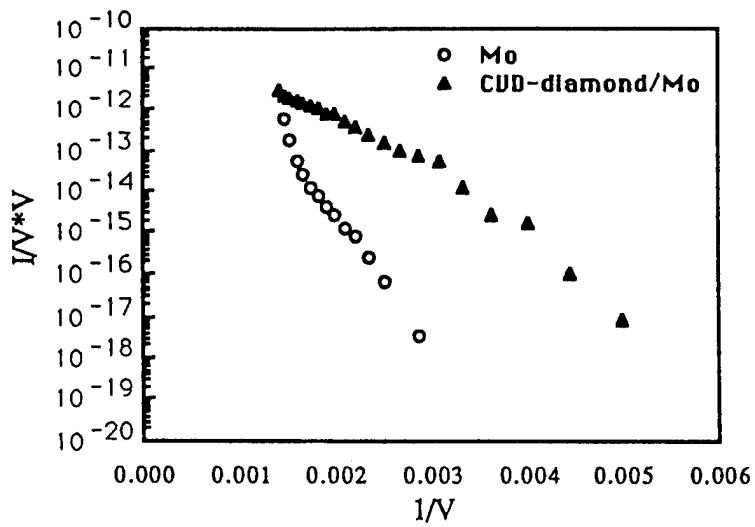
(b)

Figure 7.   (a) I-V curves for the Mo(1) emitter before and after CVD diamond coating; (b) Fowler-Nordheim plots for the same emitter.

8

(b)

(a)

Figure 8.   (a) I-V curves for the Mo(2) emitter before and after dielectrophoresis diamond powder coating; (b) Fowler-Nordheim plots for the same emitter.

Table I. Measured and effective emission parameters for the Mo(1) and Mo(2)
emitters before and after diamond deposition.

Specimen	Emitting area, (α) cm^2	Effective radius of curvature, $(r_{eff} = \sqrt{\alpha})$ cm	Measured radius of curvature, (r) cm
Mo(1)	2.2×10^{-13}	4.7×10^{-7}	3.0×10^{-6}
CVD diamond/Mo(1)	1.3×10^{-15}	3.6×10^{-8}	1.5×10^{-6}
Mo(2)	3.2×10^{-15}	3.1×10^{-8}	6.0×10^{-6}
Diamond powder/Mo(2)	3.3×10^{-11}	3.2×10^{-6}	3.0×10^{-6}

The effective emitting area (α) from diamond powder coated Mo(2) emitters was found to increase from 10^{-15} cm^2 to 10^{-11} cm^2 compared to a clean Mo emitter. This emitting area of pure Mo(2) is very similar to the results obtained by previous investigators on etched Mo wire.[16] After diamond powder coating, the calculated effective radius of the emitting area was found to be very close to the measured tip radius of curvature, $(3 \times 10^{-6}$ cm), which means that electrons were being emitted from the full tip surface area. A large emitting area could increase the electron emission of field emitters.

Emission Mechanisms. Several electron emission mechanisms for CVD-diamond were proposed. Xu *et al.*[9] suggested that electrons are transferred through the conduction channel formed between graphitic conductive particles. In the case of CVD-diamond, amorphous carbon surrounds tiny diamond crystallites, as shown in Fig. 3. However, in our study of the diamond powder coated emitters, no sp^2 or graphitic components were detected by TEM or Raman spectroscopy. Therefore, alternative explanations are needed. Huang *et al.*[10] suggested emission from the subband just below the conduction band. If defect concentration is significant, the electrons can be transferred through these defect states. Mousa[11] suggested Metal-Insulator-Vacuum system in which he considered tunneling of electrons through thin depletion layer at the metal/dielectric interface and field-induced hot-electron emission mechanism. However, if we consider an undoped or lightly doped diamond layer, the band bending effect at the metal-diamond interface is very small and can be neglected. The energy barrier height at the metal/diamond(intrinsic) interface is ~$E_g/2$. If we assume the NEA of diamond surface, then the emission would depend only on tunneling of electrons through the Mo/Diamond schottky barrier. The resultant energy band diagram for metal/diamond/vacuum is shown in Fig. 9. The tunneling length (d) in this case is d= $E_g \varepsilon$ / 2F where ε=dielectric constant, F = applied field, D = thickness of diamond and E_g = energy band gap.
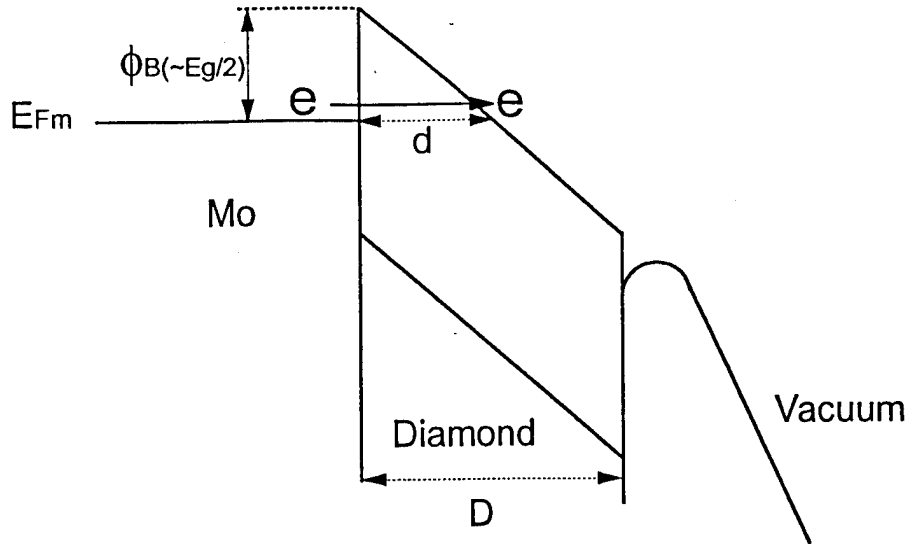
10

Figure 9.   Schematic drawing of energy band diagram for the metal/diamond/vacuum
            system.

The critical field strength (F_c) at which the bottom of conduction band of the diamond
lowered below the Fermi level of the metal is $F_c = \varepsilon\, E_g / 2D$. When a sufficiently large field
($F \gg F_c$) applied, the conduction band bottom of the diamond lowered below the Fermi level
of the metal so that the electrons will tunnel into the diamond easier. But the tunneling
thickness is still large (ε times larger). If we consider the effective work function
corresponding to this tunneling length, $\phi_{eff} = \varepsilon^{2/3}(E_g/2)$.[18,19] For the tunneling through the
metal-vacuum barrier, the effective mass of electron in the diamond $m^* = 0.2\, m_0$ should be
used.[17] The resultant effective work function $\phi_{eff} = (m^*/m_0)^{1/2}\,(E_g/2)\,\varepsilon^{2/3}$. The calculated
value is $\phi_{eff} = (0.2)^{1/2} \cdot (5.4\ eV/2) \cdot 5.6^{\,2/3} = 3.8eV$. This value is smaller than the effective
work function of metal/diamond interface($5.6^{\,2/3} \cdot (5.4\ eV/2)=8.5eV$). From this calculation
the effective work function reduced after diamond coating and the lower turn-on voltage and
high emissivity are attributed to this mechanism.

D. Summary

In this article, we have presented field emission characteristics of two different type
diamond coated Mo single emitters. CVD-diamonds were formed by the scratching method and
diamond powders were coated through dielectrophoresis. Diamond coated emitters have shown
significant increase in electron emission and lower turn-on voltage as compared to uncoated
pure Mo emitter. A large emitting area also revealed on the diamond powder coated Mo emitter.
A possible mechanism to explain the current enhancement was suggested to be electron
tunneling through diamond by field penetration and reduced effective work function.

11

E. Acknowledgments

The authors wish to thank A. T. Sower and R. J. Nemanich for performing the Raman spectroscopy.

F. References

1. I. Brodie and P. R. Schwoebel, Proceedings of the IEEE **82**, No. 7, July 1994.
2. I. Brodie and C. A. Spindt, Advances in Electronics and Electron Physics **83**, (1992).
3. J. Liu, V. V. Zhirnov, A. F. Myers, G. J. Wojak, W. B. Choi, J. J. Hren, M. T. McClure, B. R. Stoner, and J. T. Glass, J. Vac. Sci. Technol. B **13** (2), 422 (1995).
4. E. I. Givargizov, V. V. Zhirnov, A. N. Stepanova, E. V. Rakova, A. N. Kiselev and P. S. Plekhanov, Appl. Surf. Sci. **87/88**, 24 (1995).
5. W. B. Choi, J. J. Cuomo, V. V. Zhirnov, A. F. Myers and J. J. Hren, Appl. Phys. Lett., July 1995 (submitted).
6. F. J. Himpsel, J. A. Knapp, J. A. Van Vechten and D. E. Eastman, Phys. Rev. B **20**, 624 (1979).
7. J. Van der weide, Z. Zhang, P. K. Bachman, M. G. Wensell, J. Bernholc and R. J. Nemanich, Phys. Rev. B **50**, 5803 (1994).
8. N. Liu, Z. Ma, X. Chu and T. Hu, J. Vac. Sci. Technol. B **12** (3), 1712 (1994).
9. N. S. Xu, Y. Tzeng and R. V. Latham, J. Phys. D **26**, 1776 (1993).
10. Z. H. Huang, P. H. Cutler, N. M. Miskovsky and T. E. Sullivan, J. Vac. Sci. Technol. B **13**(2), 526 (1995).
11. M. S. Mousa, Sur. Sci. **266**, 110 (1992).
12. H. A. Pohl, *Dielectrophoresis*, (Cambridge University Press, Cambridge, 1978).
13. W. Zhu, C. A. Randall, A. R. Badzian and R. Messier, J. Vac. Sci. Technol. A **7**(3), 2315 (1989).
14. J. He, P. Cutler, T. Feuchtwang, N. Miskovsky and T. Sullivan, 3rd Int'l Conf. on Vacuum Microelectronics, Monterey, CA, (1990).
15. R. E. Hurley, J. Phys. D Appl. Phys. **12**, 2229 (1979).
16. C. A. Spindt, I. Brodie, L. Humphrey and E. R. Westerberg, J. Appl. Phys. **47**, 5248 (1976).
17. C. D. Clark, P. J. Dean, P. V. Harris, Proc. R. Soc. A, **277**, 312 (1964).
18. V. V. Zhirnov, W. B. Choi, J. J. Cuomo and J. J. Hren, Report at 42nd Intern. Field Emission Symposium, August 1995, Madison, WI.
19. J. G. Simmons, Phys. Rev. **166**, 912 (1968).
20. S. D. Wolter, J. T. Glass and B. R. Stoner, J. Appl. Phys. **77** (10), 15 (1995).

III. Electron Emission Measurements from CVD Diamond Surfaces*

S. P. Bozeman, P. K. Baumann, B. L. Ward, M. J. Powers, J. J. Cuomo, R. J. Nemanich
Department of Materials Science and Engineering and Department of Physics,
North Carolina State University, Raleigh, NC 27695-7919 USA

D. L. Dreifus
Kobe Steel USA Inc, Electronic Materials Center, P.O. Box 13608
Research Triangle Park, NC 27709 USA

Electron emission measurements are reported on diamond films synthesized by chemical vapor deposition. Ultraviolet photoemission spectroscopy indicates that the samples exhibit a negative electron affinity after exposure to hydrogen plasma. Secondary electron emission yields vary from 2.2 to 9.2. Field emission current-voltage measurements indicate threshold voltages ranging from 28 to 84 V/μm and effective emission barrier heights from 0.15 to 0.33 eV. The film with the highest secondary yield also exhibits the lowest emission threshold.

A. Introduction

The electron emission properties of diamond make it an attractive material for cold cathode applications such as high power, high frequency electronic devices, flat panel displays, and electron multipliers[1, 2]. Among these properties is a negative electron affinity (NEA) which has been observed on both (111) and (100) surfaces of type IIb bulk diamond and on homoepitaxial films[3, 4]. In general, electron emission studies have used ultraviolet photoemission spectroscopy (UPS), secondary electron emission (SEE), or field emission (FE), but comparison between these three types of electron emission characterization techniques has been limited. In this study we employ all three types of characterization techniques (UPS, SEE, and FE) to examine chemical vapor deposited (CVD) diamond films on silicon. Photoemission and secondary emission are similar techniques in that they generate both electrons and holes in nearly equal numbers and electron emission clearly originates from the conduction band. In an ideal field emission measurement only electrons participate and electron emission occurs from the conduction band as well. However, for p-type semiconductors it is possible that emission occurs from the valence band and holes transport through the semiconductor. Thus it is of interest to investigate correlations between the other measurements and field emission.

B. Experimental

The samples examined were diamond films grown on silicon via microwave plasma chemical vapor deposition. The study included four films ranging from insulating to highly conductive and varying in surface morphology. The films were characterized using standard scanning electron microscopy, Raman spectroscopy, and secondary ion mass spectroscopy techniques. The properties of the films are listed in Table I, including thickness, atomic boron concentration, surface morphology, and Raman FWHM.

Table I. Description of CVD diamond films used in this study.
Boron content was measured using SIMS.
The boron content of sample C was below the SIMS detection limits.

Sample	Thickness (μm)	Boron Content (cm^{-3})	Surface Morphology	Raman FWHM (cm^{-1})
A	3.2	1.1×10^{18}	(110) texture	9.4
B	4.2	1.2×10^{18}	(110) texture	6.5
C	5.8	•	(110) texture	6.6
D	4.3	3.7×10^{18}	mix of large and small grains	5.7

The first type of electron emission measurement employed was UPS. In UPS, ultraviolet light incident on the sample excites electrons from the valence band into the conduction band[5]. Electrons with sufficient energy to overcome the electron affinity of the material are emitted into the vacuum. The energy spectrum of the emitted electrons is a convolution of the valence band density of states and the conduction band density of states. As a result, UPS is typically used as a probe of the valence band density of states; thus only the higher energy portion of the photoelectron spectrum is presented. However, for a semiconductor with a NEA surface, a distinctive peak may be observed at the lowest kinetic energy in the spectra[6]. This low energy feature corresponds to the large number of secondary and scattered electrons that have thermalized to the conduction band minimum and escape into vacuum. UPS can also be used quantitatively to determine the electron affinity of a material by measuring the width of the spectrum from the valence band turn-on to the low energy cut-off. If the electron affinity is positive, this width is given by $W = h\nu - E_g - \chi$, where $h\nu$ is the excitation energy, χ is the electron affinity and E_g is the band gap. If the electron affinity is negative, then $W = h\nu - E_g$ and the magnitude of the electron affinity cannot be determined from the spectrum.

14

UPS measurements were performed in a UHV chamber (base pressure $< 2 \times 10^{-10}$ Torr) connected *in vacuo* to a hydrogen plasma system for wafer cleaning. Excitation in this system is provided by 21.2 eV (He I) light from a He resonance discharge lamp and a hemispherical analyzer is used to measure the energy spectrum of the photoemitted electrons. The sample was biased at -3 V with respect to the analyzer to allow the electrons to overcome the work function of the analyzer and facilitate the measurement of low energy electrons. The UPS system is described in more detail elsewhere[4]. UPS measurements were made of the diamond films under three conditions: 1) as-loaded, 2) after a hydrogen plasma exposure to clean and hydrogen terminate the surface, and 3) after annealing in UHV at 1000°C for 10 minutes. In step 2, the samples were exposed to a remote hydrogen plasma at a sample temperature of 500°C and H_2 pressure of 50 mTorr.

Secondary electron emission involves the ejection of low energy electrons from a surface which is exposed to a primary energetic beam of electrons[7]. The kinetic energy distribution of the emitted secondary electrons typically peaks at approximately 5 eV, with a tail generally extending no further than 20 to 30 eV. The secondary electron yield of a material is defined as the ratio of the total number of secondary electrons ejected per incident primary electron. The secondary electron yield generally depends on both the penetration depth of the primary beam and the escape depth of the secondary electrons.

Secondary electron emission measurements were obtained with the samples in a separate high vacuum chamber (pressure $< 10^{-5}$ Torr). A primary beam current of 250 nA was applied over a 1 mm diameter spot for a current density of approximately 32 $\mu A/cm^2$ and the primary beam energy was varied from 0.5 to 1.25 keV. The primary beam current (I_p) was measured by directing the beam into a Faraday cup and both the secondary electron current (I_c) and the current drawn by the sample mount (I_m) were measured by deflecting the beam into a separate enclosure containing the sample [8]. The collector which draws the secondary electron current is biased at +30 volts with respect to the sample mount to ensure collection of all emitted secondary electrons. The secondary electron yield is calculated as the ratio I_c/I_p and the equality $I_p = I_c + I_m$ can be verified for consistency. The secondary electron yield was determined at five incident energies for each of the samples.

Field emission measurements were obtained within a third high vacuum chamber (pressure $< 10^{-5}$ Torr). During the experiment, samples were placed beneath a 2 mm diameter movable platinum anode with a flat tip. The current-voltage (I-V) measurements were taken at several distances ranging from 2 to 20 μm and for bias voltages in the range of 0 to 1100 volts.

C. Results and Discussion

UPS spectra of the CVD diamond films were measured as-loaded, after a hydrogen plasma clean, and after annealing. The UPS spectra for samples A and B did not vary substantially

between the three treatments except for a small increase in the width of the spectrum after the H-plasma clean as would be expected from hydrogen surface termination. The spectra for samples C and D varied significantly in intensity and exhibited shifts of about 1 eV indicative of charging. All post-annealing spectra have widths which are consistent with NEA. The spectra for sample A are shown in Fig. 1; the results for all four samples are summarized in Table II. Some of the spectral widths are greater than hv - E_g, suggesting emission within the band gap. Two possible explanations for these spectral widths are the exciton effects discussed by Pate[9] and variations in the surface Fermi level of these polycrystalline films.
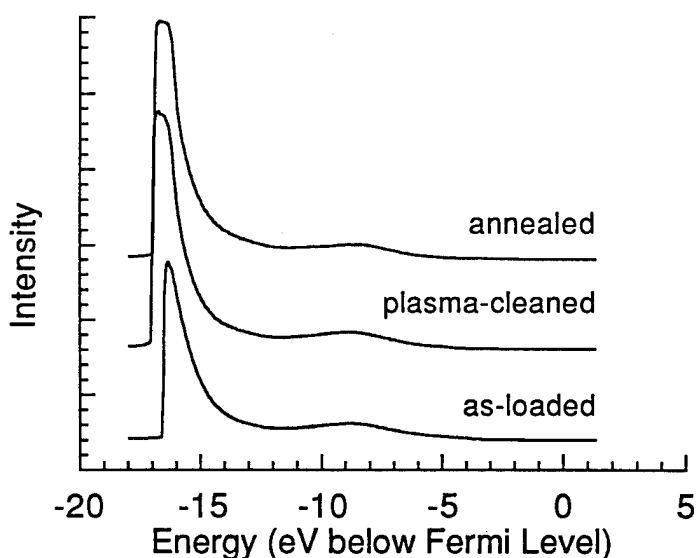

Figure 1.   UPS spectra for sample A as-loaded, after a hydrogen plasma clean, and post-annealing. The hydrogen plasma exposure induces a negative electron affinity which causes the spectrum to widen.

The measured secondary emission yields ranged from 2.0 to 9.2 between the different samples. The yields are shown in Fig. 2 as a function of energy, and peak yields are given in Table II. For each sample, the yield decreased from the peak value within minutes. Possible explanations for the decrease are removal of the hydrogen termination or electron beam effects such as surface graphitization or electron beam induced deposition. The secondary yield was independent of beam energy over the energy range covered. This result is in contrast to the reports of SEE energy dependence for Cs coated GaAs NEA emitters for which the yield increases with beam energy [10]. The lack of energy dependence of the secondary yield could be caused by a short electron diffusion length. It is known that electron transport properties are affected by grain boundaries in polycrystalline films[11]. The grain boundaries may also result in a short electron diffusion length.
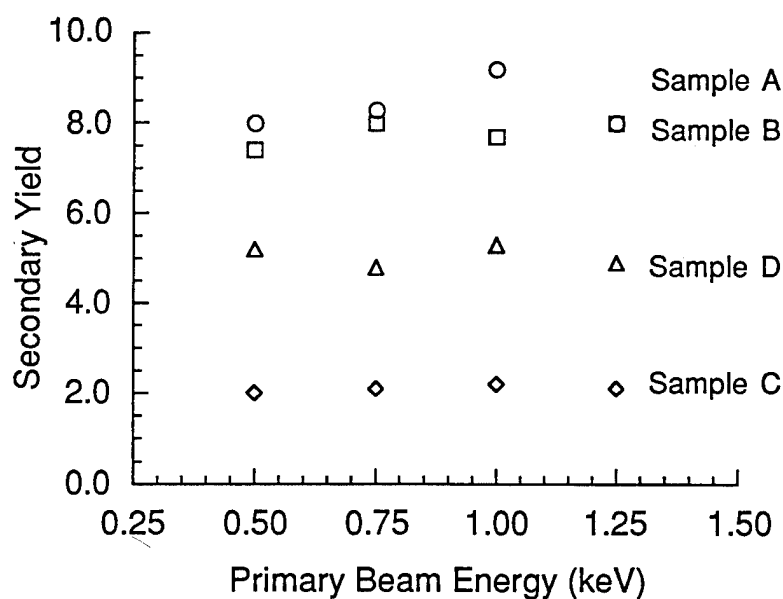
16

Figure 2.   Secondary electron yield as a function of incident beam energy for samples A, B, C, and D.

Table II. Summary of electron emission results.

W = width of UPS spectra, χ = electron affinity, and E_g = band gap of diamond = 5.45 eV. The values given for the emission threshold and barrier height are the averages and standard deviations of the measurements at different distances.

Sample	UPS as loaded	UPS plasma-cleaned	UPS annealed	Peak SEE yield	Field Emission Threshold (V/μm)	Barrier Height (eV)
A	W=15.0eV PEA, χ=+0.7	W=15.6eV PEA, χ=0.1	W=15.9eV NEA, χ<0	9.2	28 ± 2	0.16 ± 0.04
B	W=14.6eV PEA, χ=+1.1	W=15.9eV NEA, χ<0	W=16.3eV NEA, χ<0	8.6	84 ± 26	0.33 ± 0.12
C	W=13.1eV PEA, χ=+2.6	W=14.1eV PEA, χ=+1.6	W=15.7eV NEA, χ<0	2.2	43 ± 17	0.15 ± 0.01
D	Weak Signal	W=15.2eV PEA, χ=+0.5	W=15.8eV NEA, χ<0	5.3	44 ± 2	0.19 ± 0.03

Field emission I-V curves were measured for each of the four samples. Emission thresholds were estimated by the electric field at which the current exceeded 0.1 μA. This method yielded threshold fields ranging from 28 to 84 V/μm which are summarized in Table II. These threshold values are consistent with values reported for diamond by other authors [12]. The maximum current drawn in typical measurements was 1 μA, equivalent to 32 μA/cm^2 if one assumes the entire area under the anode is emitting. The values listed in Table II are the averages and standard deviations of the measurements at the different distances. The threshold fields at different distances agreed well for samples A and D, while the other samples exhibited more scatter. Possible sources of the scatter are variations in distance caused by vibration and changes in the density of emitting sites. Other reports have indicated that the emitting sites are a small fraction of the total film surface, making the true current density difficult to estimate[13]. Field emission I-V curves for sample A are shown in Fig. 3 for six distances.
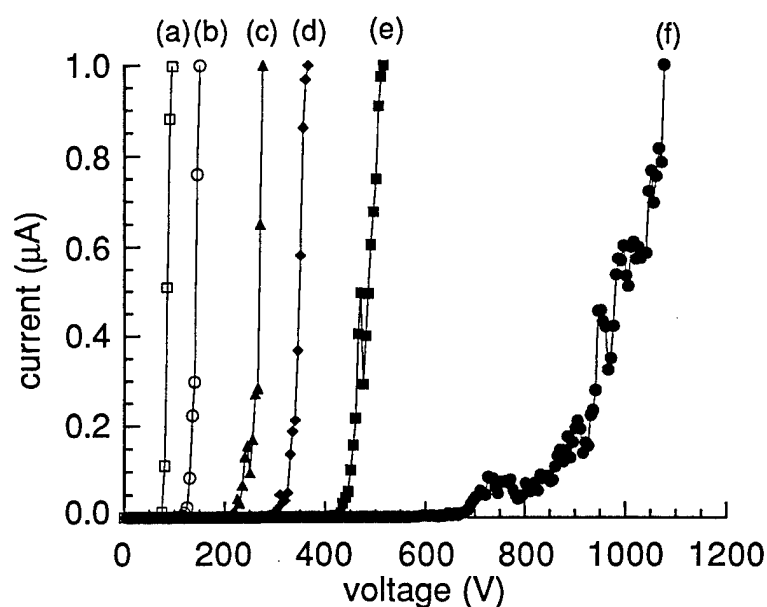

Figure 3.   Field emission I-V curves for sample A at distances of (a) 2.6μm, (b) 5.3μm, (c) 8.8μm, (d) 11.4μm, (e) 15.8 μm and (f) 19.8μm. The threshold electric fields from these curves are averaged to give the threshold value in Table II.

These field emission results can be analyzed in terms of Fowler-Nordheim theory describing emission via barrier tunneling[14]. The Fowler-Nordheim equation has the form,

$$I = k\left(\frac{V}{d}\right)^2 \exp\left(\frac{-6530d\phi^{3/2}}{V}\right)$$ (1)

where k is a constant, V is the voltage in volts, φ is the barrier height in eV, and d is the distance from the anode to cathode in microns. Figure 4 is a plot of I/V^2 vs. $1/V$ for sample A. The straight lines are fits to Eq. 1, and are used to determine values for the effective barrier heights which are given in Table II. This analysis neglects the field enhancement factor, in effect assuming that the surface is perfectly flat. Surface roughness will tend to increase the field strength, leading to an underestimation of the actual barrier height in this analysis.
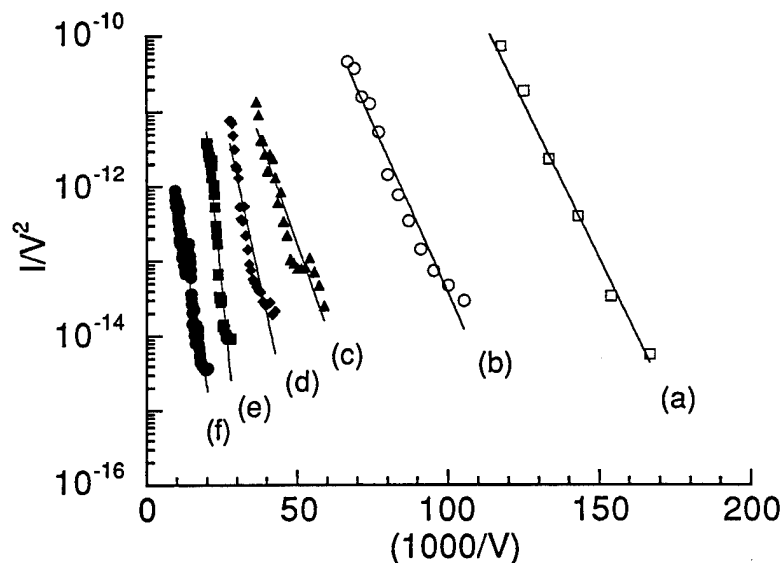

Figure 4.   Fowler-Nordheim plot of field emission I-V data presented in Figure 5. The slopes of the lines fit to these data are used to derive the effective barrier heights using equation (1).

Samples A and B which have the highest SEE yields also have the most robust UPS signals, while sample C had the lowest yield and the weakest UPS signal. Sample C was also the only one of the samples that was insulating (see Table I). The low conductivity of sample C may also explain the low secondary yield as charging of the diamond surface would reduce the emission of the low energy secondary electrons. However, sample D also has a yield which is lower than A and B but its dopant level is the highest of all. Thus, the dopant level is not the only factor determining the electron emission characteristics of the diamond. The surface of sample D contains large diamond crystals scattered on top of smaller grains. This unusual morphology may be connected with the low secondary yield. The film with the lowest field emission threshold also exhibits the highest secondary yield, but this correlation is not continued in the other three samples. This preliminary analysis of the field emission contains several assumptions which should be examined in more detail. Specifically, it neglects the effects of surface morphology, possible changes in the density of emitting sites, and the

presence of adsorbates or other surface contamination. In addition, since the samples were exposed to air between the different emission measurements, it is unclear whether the surface properties measured by UPS hold for the other techniques.

D. Conclusions

Results of electron emission measurements are reported for CVD diamond films. Ultraviolet photoemission spectroscopy indicates that the samples exhibit NEA after exposure to hydrogen plasma. Secondary electron emission yields vary from 2.2 to 9.2. Field emission I-V measurements indicate threshold voltages ranging from 28 to 84 V/μm and emission barriers from 0.15 to 0.33 eV. Preliminary results indicate a complex combination of excitation, transport, and emission processes. Additional samples of various types need to be evaluated and compared in order to understand these mechanisms.

E. Acknowledgments

F. References

1. M.W. Geis, N. N. Efremow, J. D. Woodhouse, M. D. McAleese, M. Marchywka, D. G. Socker and J. F. Hochedez, IEEE Electron Device Letters, **12** (1991) 456.
2. G. T. Mearini, I. L. Krainsky, J. A. Dayton, Y. Wang, C. A. Zorman, J. C. Angus and R. W. Hoffman, Applied Physics Letters, **65** (1994) 2702.
3. F. J. Himpsel, J. A. Knapp, J. A. van Vechten and D. E. Eastman, Physical Review B, **20** (1979) 624.
4. J. van der Weide, Z. Zhang, P.K. Baumann, M.G. Wensell, J. Bernholc and R.J. Nemanich, Physical Review B, **50** (1994) 5803-5806.
5. A. Zangwill, *Physics at Surfaces*, Cambridge University Press, Cambridge, 1988.
6. B. B. Pate, W. E. Spicer, T. Ohta and I. Lindau, Journal of Vacuum Science and Techology, **17** (1980) 1087.
7. A. Modinos, *Field, Thermionic, and Secondary Electron Emission Spectroscopy*, Plenum Press, New York, 1984.
8. M. J. Powers, Photoemission From BN and Secondary Electron Emission From Negative Electron Affinity Surfaces, North Carolina State University, M.S. Thesis (1995).
9. C. Bandis and B. B. Pate, Physical Review Letters, **74** (1994) 777-780.
10. R. U. Martinelli and D. G. Fisher, Proceedings of the IEEE, **62** (1974) 1339-1360.
11. J. Y. W. Seto, Journal of Applied Physics, **46** (1975) 5247.
12. W. Zhu, G. P. Kochanski, S. Jin and L. Siebles, Journal of Applied Physics, (1995) in press.
13. N. S. Xu, R. V. Latham and Y. Tzeng, Electronics Letters, **29** (1993) 1596.
14. R. Gomer, *Field Emission and Field Ionization*, Harvard University Press, Cambridge, Massachusetts, 1961.

IV. Distribution List

Mr. Max Yoder   3
Office of Naval Research
Electronics Division, Code: 312
Ballston Tower One
800 N. Quincy Street
Arlington, VA 22217-5660

Administrative Contracting Officer   1
Office of Naval Research
Regional Office Atlanta
101 Marietta Tower, Suite 2805
101 Marietta Street
Atlanta, GA 30323-0008

Director, Naval Research Laboratory   1
ATTN: Code 2627
Washington, DC 20375

Defense Technical Information Center   2
Bldg. 5, Cameron Station
Alexandria, VA 22314